

Performance Comparison between Decawave DW1000 and DW3000 in low-power double side ranging applications

Tommaso Polonelli
D-ITET
ETH Zurich
Zurich, Switzerland
0000-0002-6134-7310

Simon Schl pfer
D-ITET
ETH Zurich
Zurich, Switzerland
0000-0003-0405-3612

Michele Magno
D-ITET
ETH Zurich
Zurich, Switzerland
0000-0003-0368-8923

Abstract—Indoor localization and context-awareness are becoming two of the key technologies for a large variety of applications. Real-time locating systems with centimeter accuracy and low power consumption have recently been made available by employing the Ultra WideBand (UWB) technology. Since 2015, Decawave has produced commercial UWB integrated circuits, exploiting time-of-flight measurement techniques to estimate the distance between two agents. This work presents a performance study between two Decawave transceivers, the DW1000 and the new DW3000 released in 2020. The testing space includes areas under line-of-sight and diverse non-line-of-sight conditions caused by the reflection of the UWB radio signals across various obstacles. Finally, we analyze the power consumption in distinct configurations, comparing the two devices. Results show that the two have similar precision in measurement ranges above one meter, while the DW3000 performs, on average, 33.2% better considering shorter distances. Moreover, the new transceiver features reduced power consumption by almost 50% during real-time measurements reaching an average value of 55 mW.

Index Terms—Ultra wideband technology, Ultra wideband communication, IoT, Indoor Localization, Power Consumption

I. INTRODUCTION

Today, accurate indoor localization for low power and mobile devices is still an open problem [1]. In the Internet of Things (IoT) ecosystem, context and environmental awareness have been recognized as fundamental properties [2]. Within all the application scenario details, relative and absolute location information, among other items, plays important roles [3]. Many approaches have been proposed to obtain usability similar to other outdoor technologies, such as GPS and GNSS [3]. However, today there is no ready-to-use solution for indoor low power localization, leaving this challenging research topic still unsolved. In recent years, researchers and companies have invested heavily to enable indoor location awareness, developing a significant amount of prototypes and the first commercial solutions in IoT [2]. The most difficult challenge for indoor positioning is to find an accurate-enough indoor location method [4], valid for extended areas, robust to changes to environmental conditions, scalable to support thousands of devices [5], and at the same time to decrease the energy

consumption [6]. Since in IoT a wireless radio link is a crucial prerequisite, the usage of radio waves for indoor localization is becoming more and more preferable, especially when the same interface enables data transfer and localization [6]. Multiples approaches, based on commonly named Angle of Arrival (AoA), Phase of Arrival (PoA), Time of Flight (ToF), Time Difference of Arrival (TDoA), and Return Time of Flight (RToF) are showing improved performance for IoT indoor localization. The first two, AoA and PoA, require an array of antennas, limiting the compactness of the designed solution, while the rest need a single antenna and a radio-frequency transceiver [1].

Ultra-WideBand (UWB) is a pivotal technology to solve many challenges related to the Real-Time Location (RTL) of objects in GPS-denied areas. UWB is computationally lightweight and allows to localize objects with centimeter, or even sub-centimeter [7] accuracy, while being energy-efficient [8]. Especially, Decawave's DWM1000 is widely used in many research and commercial solutions [6], [7], [9]. It is a commercial UWB integrated circuit (IC) that supports time-of-flight (ToF) measurement and RToF protocols to accurately estimate the distance among generic devices. Moreover, TDoA is reinforced by adding an extra software layer. With the distances between one node and at least four anchors, a trilateration algorithm can be applied to estimate its location in two-dimensional (2D) and three-dimensional (3D) space. However, recent researches [6], [9] have shown that the ranging accuracy (i.e., under 30 cm range, in non-line-of-sight, or in the presence of external electromagnetic noise) of the DW1000 is still not reliable in several conditions. Thus, essential tasks, such as precision indoor navigation, are still challenging. Recently, a new UWB transceiver by Decawave was introduced. It claims to improve energy efficiency and ToF accuracy.

This work presents a performance comparison between Decawave DW1000 and Decawave DW3000 in real and heterogeneous application scenarios. We compared the two modules in identical conditions and at the same time to avoid any bias caused by external interference. The assessment is

performed in different environments, in line-of-sight, with no direct visibility between two devices to force the generation of reflection and moving objects. Our tests show that the module behavior is comparable in ideal conditions, while the DW3000 performs better in short distances, under 30 cm, featuring a standard deviation reduced of 33% concerning its predecessor. Moreover, it also shows a root mean square error indicator reduced by 71% on average. A similar attitude is verified in non-ideal antenna orientation, e.g., horizontal position. The power consumption and the energy per measurement are investigated. We verified that the new DW3000 provides an average power consumption of 50% lower than the DW1000, with an absolute value of 55 mW and a peak of 160 mA during the reception. This work can drive future researchers and engineers to the optimal module selection for many different IoT applications, especially where a wireless link and a low power indoor localization are leading requisites.

II. RELATED WORKS

In 2014, Decawave released the DW1000, the world's first integrated circuit UWB transceiver. It enabled the development of cost-effective and compact RTLS solutions with precise indoor and outdoor positioning, promising a final ranging accuracy within ± 10 cm. In recent years, DW1000 is exploited in many commercial and scientific projects, ranging from low-power wearable indoor localization [9], vehicle localization for distributed path planning [10], industry automation [11], real-time drone localization with base-stations [6], [9] and, even more complex frameworks with swarm of drones [12]. It is *de facto* the technology leader in low power indoor awareness compared to other solutions, such as Ubisense, Bespoon and the NXP Trimension series [13]. Moreover, UWB technology is already featured in the last generation of smartphones, which is expected to support indoor localization at a centimeter-level along with high-speed data transfer. Based on IEEE802.15.4-2011, the DW1000 can also support IoT applications, supporting up to 6.8 Mbps in point-to-point data streaming. Even though 3D and 2D localization methods and scalability have been investigated in the literature, the real positioning precision and the power consumption are still open challenges in the IoT field [8]. Indeed, in reception mode, the DW1000 reaches up to 600 mW, a value often not sustainable for ultra-low power devices.

Authors like Dardari *et al.* modeled the UWB performances [4] in line-of-sight (LOS) and non-line-of-sight (NLOS) conditions, while in [14] results show an indoor localization precision around 10 cm with fixed objects. However, the literature shows a performance drop for in-field application scenarios with moving objects and external background noise. The results of several previous works [6], [9], [15]–[19] show that the UWB ranging accuracy provided by DW1000, despite its high reliability in ideal conditions, can be affected by many factors. For example, NLOS and multi-path radio propagation lead to erroneous and spurious measurements, other than LOS biases relative to the antenna radiation pattern [19].

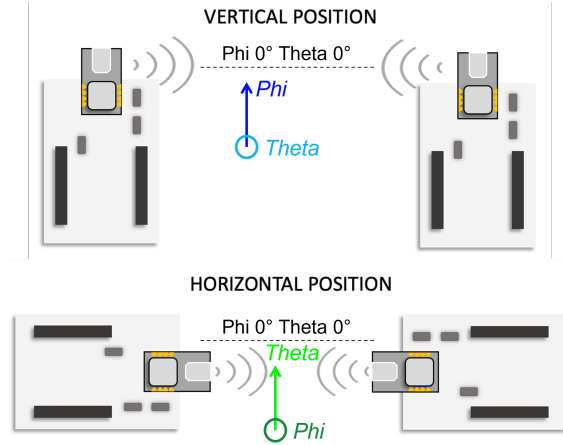


Fig. 1. Vertical and horizontal positions of the UWB sensors and their shield. Theta and Phi are relative to the antenna radiation pattern.

The new recent state-of-the-art UWB IC series by Decawave, DW3000, was released on the market. Today, few papers and scientific works characterize the new transceiver in terms of power consumption and ranging accuracy, such as [20]. However, to the best of our knowledge, there are no technical comparisons between the well-known DW1000 and the new DW3000.

III. HARDWARE SETUP

This chapter describes the hardware implementation used to compare the DW1000 with the new DW3000. We used the same microcontroller (MCU) and hardware support and, where it was possible, the same software configurations and Software Development Kit (SDK), see Table I for radio settings. For fairness in performance comparisons and to allow the replication of our results, we did not use custom hardware, exploiting only off-the-shelf components and evaluation boards. We used the modules DWM1000 and DWM3000, connected to an expansion board provided by Qorvo (DWS1000) and supported by an STMicroelectronics evaluation kit, the STM32 NUCLEO-F767ZI. At the time of writing, the DWS1000 was available only for the DWM1000, but we soldered the new transceiver on the Qorvo shield due to the pin-to-pin compatibility.

A. Relative Antenna Orientation

Since the antenna's relative orientation between two devices affects the ideal ToF estimation due to variation in RSSI and propagation delay, which is not constant concerning its radiation pattern, it is fundamental to define the 3D space position and orientation of each agent. The literature proposes two different ways how the orientation of a device can be described [21]. First, the more intuitive Euler angles, and secondly, the more sophisticated quaternions are introduced. A 3D body can be rotated about three orthogonal axes: Yaw, Pitch, and Roll. Since the investigation and characterization of the UWB behavior regarding moving objects and different antennas goes beyond the paper contribution, we simplified

the problem by selecting two key positions for distance measurement and module comparison. The vertical position is where the upsides look against each other, and the horizontal orientation is where the sender and receiver are in a flat position. A schematic visualization in 2D is given in Fig. 1. The modules DWM1000 and DWM3000 feature a ceramic chip antenna, respectively UWB44 and UWB06, which are vertically polarized, meaning that the module is preferable to be positioned vertically upright when used in an RTL system.

The DWM1000's datasheet provides information about the antenna radiation pattern. The UWB44 features an omnidirectional radiation pattern in the vertical position while rotating around the roll axis. This is different in the horizontal position; thus, the polarization changes with a rotation around the yaw axis. In this case, the horizontally polarized pattern applies, and there are nulls at certain angles, limiting the range and introducing location inaccuracy. At 0 and 180 degrees, there is a gain drop of more than 15 dBi. Consequently, already small rotations around the yaw axis result in gain differences and, therefore, in ranging inaccuracies.

IV. DISTANCE MEASUREMENT

In this section, the accuracy and the precision of collected distance measurements between two devices of the same type are evaluated on the Root Mean Square Error (RMSE) and the Standard Deviation (SD) parameters. This was done between two Decawave DWM1000 sensors and between two Decawave DWM3000 arranged within a precision of ± 0.5 cm. Data was collected in a LOS measurement with two different antenna orientations at several distances and in an NLOS measurement with fixed orientation and distance. Refer to the product datasheet and user manual for specific configurations, such as the channel definition and Table I. A part of low lever register setting and mapping, which differ between the two devices, the firmware and APIs are identical.

A. Line-of-Sight Measurement

The LOS experiment collected distance measurements in vertical and horizontal positions at seven different distances: 10 cm, 20 cm, 30 cm, 50 cm, 90 cm, 100 cm, and 300 cm. For each length, 2500 data points were collected, with a measurement window of 250 s. The sensor was placed 20 cm above the ground, and jumper cables connected it to the Nucleo board. Note that in an initial setup, where the antenna was placed just 1 cm above the Nucleo board, many reflections

TABLE I
CONFIGURATION OF DW1000 AND DW3000

Description	Used setting
Pulse repetition frequency	DWT_PRF_64M
Preamble length, used in TX only	DWT_PLEN_128
Preamble chunk size, used in RX only	DWT_PAC8
TX preamble code, used in TX only	9
RX preamble code, used in RX only	9
Standard SFD	0
Data rate	DWT_BR_6M8
PHY header mode	DWT_PHRMODE_STD
SFD timeout, used in RX only	(129 + 8 - 8)

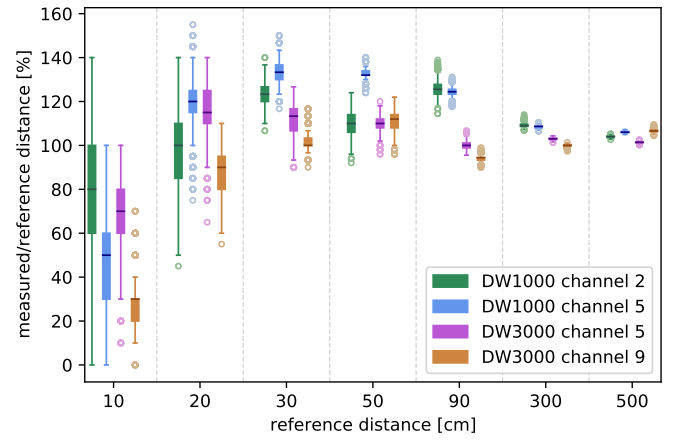


Fig. 2. LOS distance measurements in vertical position for the DW1000 and the DW3000. Plot generated by *matplotlib.pyplot.boxplot* function.

occurred and caused multipath problems. No metallic obstacles or other potential reflectors were placed between or near the two sensors.

Fig. 2 illustrates the difference between the two sensors. Overall, the spread of the ratio between measured and reference distances is bigger for low distances. However, there is a noticeably higher precision at a distance of 10 cm for measurements with the new DW3000. The SD is reduced by 33.2% (with channel 5). Channel 9 of the DW3000 generally performs better (10% offset) in ranges under 30 cm. In longer ranges, the two sensors have a similar precision. Table II shows the RMSE and the SD of the transceivers with their respective channels. Again, the DW3000 is not just more precise (smaller SD) but also more accurate (lower RMSE). Overall distances, it features a reduced RMSE of 71.3% and, the SD is also reduced by 5.5% (channel 5). The exact measurement was done with the worst antenna orientation (horizontal position). A gain of -11 dBi was observed in the horizontal position, which results in worse accuracy visible in Fig. 3. The modules were moved between each distance measurement. Moreover, a noticeable increase of the variance with respect Fig. 2 is visible, which confirms the accuracy degradation of both transceivers in this antenna location. If the board is rotated by 10 degrees, the gain changes to -3 dBi, even more highlighting measurement instability in this specific working point. Nonetheless, two main considerations can be analyzed. First, measurements obtained in the horizontal orientation have worse accuracy and precision than those obtained in the vertical direction. This is visible in the direct comparison

TABLE II
RMSE AND SD OVERVIEW IN VERTICAL POSITION

Sensor	RMSE <30 cm	RMSE tot.	SD <30 cm	SD tot.
DW1000 CH2	4.7	12.9	2.4	2.5
DW1000 CH5	6.9	16.4	2.0	1.8
DW3000 CH5	3.7	4.7	1.8	1.7
DW3000 CH9	3.9	8.4	1.3	1.8

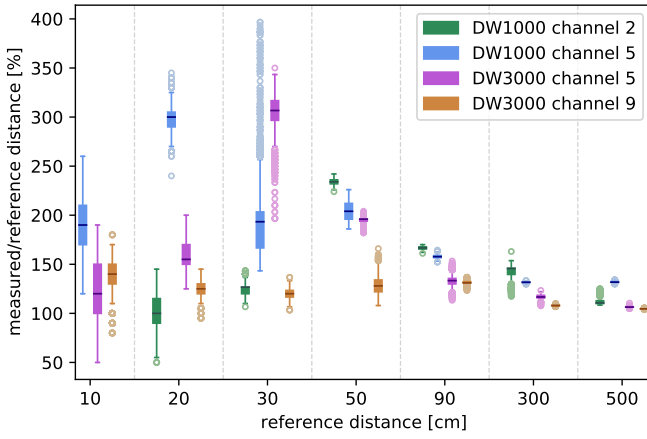


Fig. 3. LOS distance measurements in the horizontal position for the DW1000 and the DW3000. Negative distances were measured with the same configuration and calibration at 10 cm with DW1000 channel 2. This data is not included in the plot. Plot generated by *matplotlib.pyplot.boxplot* function.

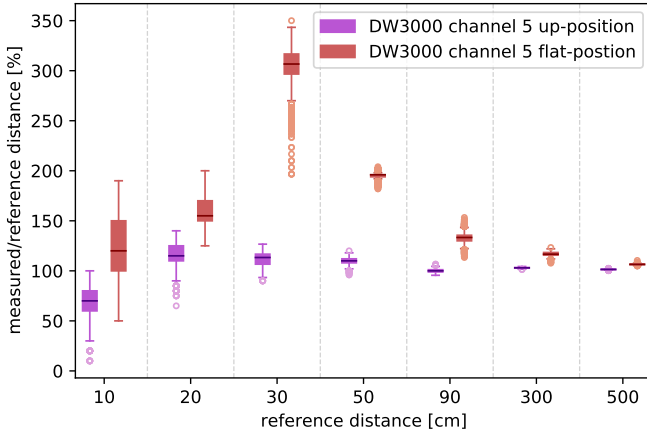


Fig. 4. Comparison of the error distribution in vertical (up) and horizontal (flat) positions. Plot generated by *matplotlib.pyplot.boxplot* function.

of measurements with channel 5 of the two orientations, see Fig. 4. Overall distances, the RMSE increased by 7, the SD by a factor of 2. Moreover, one can see that for distances above 50 cm, the percentage error of the orientation decreases in relation to the reference measure. Indeed, at 10 cm the bias is 50% of the reference, while at 5 m it is less than 7%. This is also motivated in the paper [6], which suggests other localization methods under 30 cm range. Table III shows that the new DW3000 performs better in the horizontal position than the DW1000. Channel 5 of the new sensor has a 45.7% smaller RMSE and 5.6 % smaller SD compared to channel 5 of DW1000. Especially channel 9 is more resistant in the horizontal orientation since the RMSE has increased only by a factor of 1.8, and the SD is comparable with the vertical position. Fig. 5 shows the distribution of the measured data. In comparison to Decawave's newly released datasheet of DW3000 [22], the measured data is not perfectly normally distributed. This could be due to unintentional reflections

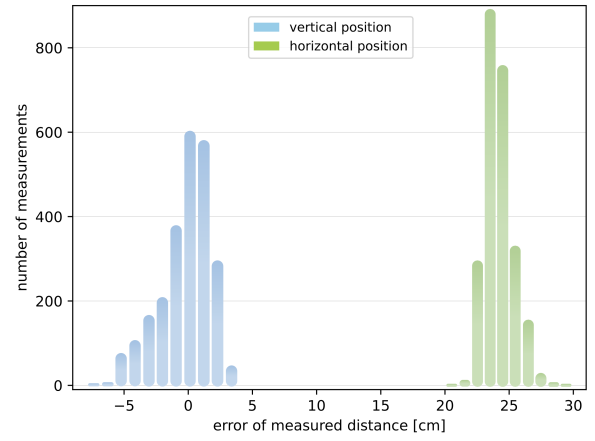


Fig. 5. Distribution of LOS measurement at 3 m with DW3000 channel 9, vertical and horizontal position.

from antenna non-homogeneity or a non-ideal environmental condition.

B. Non-Line-of-Sight Measurement

In the NLOS experiment, distance measurements were collected in the vertical position antenna direction at 3 m. Again, the sensor was placed 20 cm above the ground, and jumper cables connected it to the Nucleo board. Different moving metallic obstacles and other potential reflectors were placed between the two sensors. To ensure equal conditions, the DWM1000 and the DWM3000 were evaluated at the same time. To avoid interference, the DWM1000 was configured with Channel 5, and the DWM3000 was configured with Channel 9. Fig. 6 illustrates the impact of the metallic obstacles. The standard deviation is 15× bigger than in the LOS measurement. This accuracy drop is due to multipath channel effects, where metallic objects attenuate the direct signal path and cause reflections. Therefore, the signal reaches the receiver only via multiple reflections, and the measured ToF is affected. This is also visible in Fig. 6, where almost all measured distances are longer than in the previous LOS scenario. There is no significant and statistical difference between the two sensors. The DWM3000 has an SD of 29.0 cm compared to 29.8 cm with the old transceiver. Thus, the lower TX power of the DW3000 [22] has no impact in the chosen scenario. The distribution of the NLOS measurement (Fig. 7) slightly changed in comparison to the LOS measurement (Fig. 5). The distribution is similar, but the offset is in the range of meters, one order of magnitude bigger than in LOS. Once again, one can see that the error is almost only positive.

TABLE III
RMSE AND SD OVERVIEW IN HORIZONTAL POSITION

Sensor	RMSE <30 cm	RMSE tot.	SD <30 cm	SD tot.
DW1000 CH2	5.6	54.7	2.6	6.2
DW1000 CH5	26.9	62.8	5.8	4.0
DW3000 CH5	25.8	34.1	3.5	3.5
DW3000 CH9	5.1	15.0	1.5	1.7

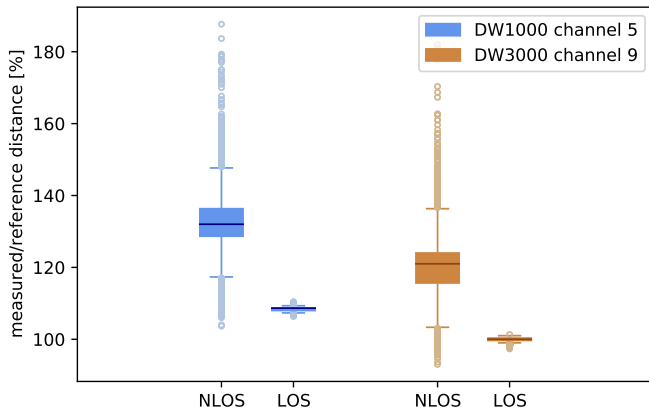


Fig. 6. Comparison of DW1000 channel 5 and DW3000 channel 9 with NLOS and LOS distance measurement at 3 m. Plot generated by *matplotlib.pyplot.boxplot* function.

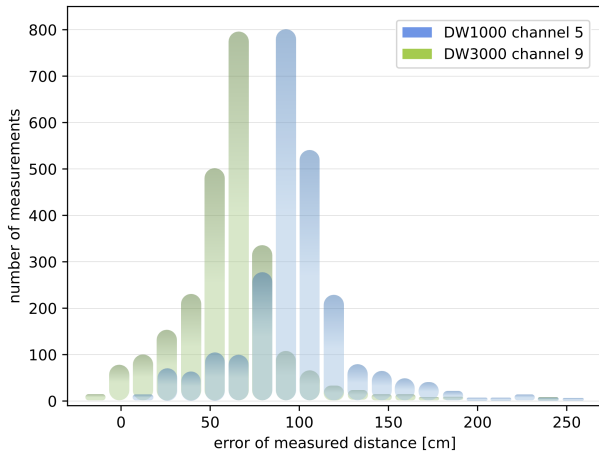


Fig. 7. Distribution of NLOS measurement with DW1000 channel 5 and DW3000 channel 9.

V. POWER CONSUMPTION MEASUREMENT

The power consumption was characterized with an N6705C DC Power Analyzer from Keysight. Together with the overall voltage of the DWS (3.3 V), all required parameters were known to calculate the power consumption of the board during a ranging cycle. A typical-ranging cycle of the initiator was measured to compare the two sensors. This was done with two channels of each module. Channel 2 & 5 for the DWM1000 and channels 5 & 9 for the DWM3000.

On Fig. 8, the three steps of the DS TWR (*Poll*, *Response*, *Final*) are visible. At the second peak, the highest power consumption is observed (DWM1000: 233 mW, DWM3000: 129 mW), which refers to the reception windows between two successive transmissions. Therefore, the power supply must be able to deliver high peak currents for short times. Moreover, Fig. 8 confirms that the new DW3000 is more energy-efficient than the DW1000. With channel 5 the average power consumption is reduced by 50%, reaching an average value of 55 mW. The average is computed considering a

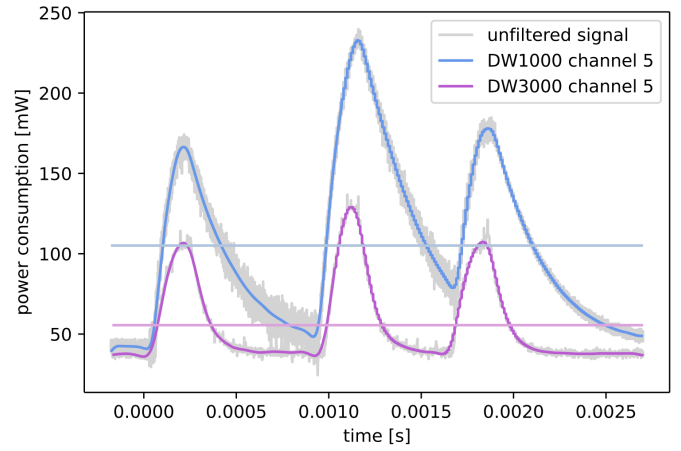


Fig. 8. Power consumption of DW1000 channel 5 and DW3000 channel 5, configured as initiator. The signals were filtered with a Butterworth filter. The straight line is the average power consumption.

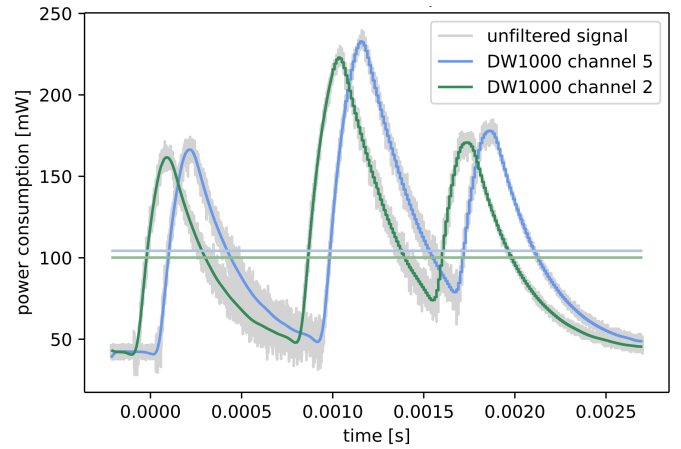


Fig. 9. Power consumption of DW1000 channel 2 and 5.

ranging window of 2.5 ms and the DS TWR messages needed to estimate the TDoA. Generally, the peak of the power consumption is mainly affected by these four parameters [22]: (i) operating channel, (ii) data rate, (iii) preamble length, (iv) pulse repetition length (PRF). The higher the frequency, the higher the power consumption. Consequently, channel 9 needs more energy than channel 5. This is visible in Fig. 10. The average power consumption is 44% higher for channel 9 than for channel 5. The two channels in Fig. 9 are purposely shifted in time to avoid a perfect overlap between them. Indeed, the difference between channel 5 and channel 2 is negligible. The data rate of both ICs is 6.8 Mbit/s. This is the highest possible data rate, in which the frames are sent in the shortest time.

To make the sensor more energy efficient, the PRF could be modified to 16 MHz. However, the impact would be marginal [22]. For comparing the two modules, the default configuration of 64 MHz remained unchanged. There are additional possibilities to save power. Decawave provides low power states like *OFF*, *SLEEP* and *DEEPSLEEP*. Nonetheless, the startup time to return to TX/RX operational mode is about

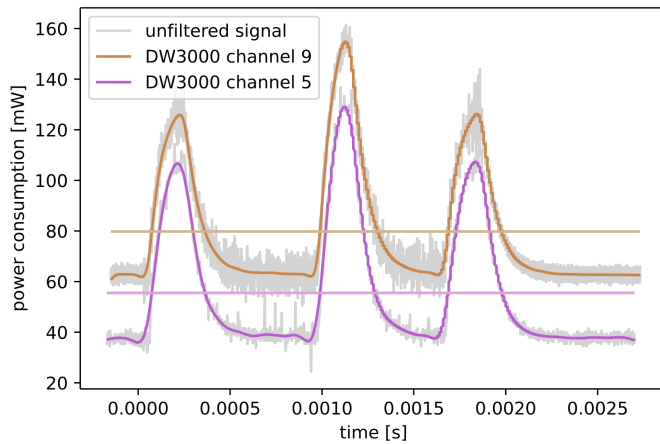


Fig. 10. Power consumption of DW3000 channel 5 and 9.

5 ms. The impact could be rather low for applications where high localization frequencies are desirable. To optimize the receive mode, one could use the SNIFF MODE where the IC switches automatically between high power modes to low power states [22].

VI. CONCLUSION

This paper has presented a point-to-point comparison between two DecaWave ICs, the DW1000, and the DW3000. Power consumption and distance estimation are modeled in different environmental conditions and by varying radio-frequency settings. Background observations and hardware-firmware setup are precisely reported, allowing the replication of our tests and the future implementation of our model for error correction algorithms in a wide span of application scenarios. Results suggest that the DW3000 generally performs better than its counterpart. In LOS conditions, it is more precise, reduced SD of 5.5%, and more accurate, RMSE decreased 71%. On average, it features a distance accuracy that is constantly under 10 cm in LOS and optimal antenna orientation. On the other hand, NLOS performances are comparable; indeed, the improved DW3000 hardware has no impact in this scenario, where radio-frequency reflections generate the majority of the measurement uncertainty. Finally, the DW3000 features a decreased power consumption with a factor of $2\times$ concerning its predecessor and a current peak decreased of 45%—an ideal requirement for any IoT low power device.

ACKNOWLEDGMENT

This work was partially supported by the Swiss National Science Foundation (SNSF) Bridge Project “AeroSense” under Project 40B2-0_187087. Moreover, authors are grateful to Vlad Niculescu for the technical support.

REFERENCES

- [1] H. Obeidat *et al.*, “A review of indoor localization techniques and wireless technologies,” *Wireless Personal Communications*, pp. 1–39, 2021.
- [2] F. Zafari *et al.*, “A survey of indoor localization systems and technologies,” *IEEE Communications Surveys & Tutorials*, vol. 21, no. 3, pp. 2568–2599, 2019.
- [3] L. Chen *et al.*, “Robustness, security and privacy in location-based services for future iot: A survey,” *IEEE Access*, vol. 5, pp. 8956–8977, 2017.
- [4] W. Gifford *et al.*, “The impact of multipath information on time-of-arrival estimation,” *IEEE Transactions on Signal Processing*, 2020.
- [5] M. Zhao *et al.*, “Uloc: Low-power, scalable and cm-accurate uwb-tag localization and tracking for indoor applications,” *Proceedings of the ACM on Interactive, Mobile, Wearable and Ubiquitous Technologies*, vol. 5, no. 3, pp. 1–31, 2021.
- [6] T. Polonelli *et al.*, “A flexible, low-power platform for uav-based data collection from remote sensors,” *IEEE Access*, vol. 8, pp. 164 775–164 785, 2020.
- [7] S. Pala *et al.*, “A leading edge detection algorithm for uwb based indoor positioning systems,” in *International Conference on Ubiquitous Communications and Network Computing*. Springer, 2021, pp. 45–55.
- [8] T. Polonelli, “Ultra-low power iot applications: from transducers to wireless protocols,” 2021.
- [9] P. Mayer *et al.*, “Embeduwb: Low power embedded high-precision and low latency uwb localization,” in *2019 IEEE 5th World Forum on Internet of Things (WF-IoT)*. IEEE, 2019, pp. 519–523.
- [10] R. Mocanu *et al.*, “Indoor and outdoor vehicle localization using uwb transceivers,” in *2019 27th Mediterranean Conference on Control and Automation (MED)*. IEEE, 2019, pp. 299–303.
- [11] Y. Dobrev *et al.*, “Steady delivery: Wireless local positioning systems for tracking and autonomous navigation of transport vehicles and mobile robots,” *IEEE Microwave Magazine*, vol. 18, no. 6, pp. 26–37, 2017.
- [12] J. A. Preiss *et al.*, “Crazyswarm: A large nano-quadcopter swarm,” in *2017 IEEE International Conference on Robotics and Automation (ICRA)*. IEEE, 2017, pp. 3299–3304.
- [13] A. R. J. Ruiz *et al.*, “Comparing ubisense, bespoon, and decawave uwb location systems: Indoor performance analysis,” *IEEE Transactions on Instrumentation and Measurement*, vol. 66, no. 8, pp. 2106–2117, 2017.
- [14] M. Malajner *et al.*, “Uwb ranging accuracy,” in *2015 International Conference on Systems, Signals and Image Processing (IWSSIP)*. IEEE, 2015, pp. 61–64.
- [15] W. Zhao *et al.*, “Learning-based bias correction for ultra-wideband localization of resource-constrained mobile robots,” 03 2020.
- [16] H. Wymeersch *et al.*, “A machine learning approach to ranging error mitigation for uwb localization,” *IEEE Transactions on Communications*, vol. 60, no. 6, pp. 1719–1728, 2012.
- [17] A. Ledergerber *et al.*, “Calibrating away inaccuracies in ultra wideband range measurements: A maximum likelihood approach,” *IEEE Access*, vol. 6, pp. 78 719–78 730, 2018.
- [18] A. Poulou *et al.*, “Uwb indoor localization using deep learning lstm networks,” *Applied Sciences*, vol. 10, p. 6290, 09 2020.
- [19] W. Zhao *et al.*, “Learning-based bias correction for ultra-wideband localization of resource-constrained mobile robots,” *arXiv preprint arXiv:2003.09371*, 2020.
- [20] S. Ruponen *et al.*, “Trusted radionavigation via two-way ranging,” in *Proceedings of the 2021 International Technical Meeting of The Institute of Navigation*, 2021, pp. 525–538.
- [21] C. De Farias *et al.*, “Dual quaternion-based visual servoing for grasping moving objects,” in *2021 IEEE 17th International Conference on Automation Science and Engineering (CASE)*. IEEE, 2021, pp. 151–158.
- [22] DW3000 User Manual, May 2021.